Acoustic barriers and observation of guided elastic waves in GaN-AlN structures by Brillouin scattering

M. Chirita and R. Sooryakumar
Department of Physics, The Ohio State University, Columbus, Ohio 43210

R. Venugopal, J. Wan, and M. R. Melloch
School of Electrical and Computer Science, Purdue University, West Lafayette, Indiana 47907

(Received 25 September 2000; published 12 April 2001)

We report on the localization of acoustic waves in GaN-AlN heterolayers deposited on Si that lead to the observation, by Brillouin light scattering, of distinctive guided excitations associated with the hexagonal ($2H$) GaN epilayers. These elastic modes include the longitudinal guided resonance (LGR) propagating parallel to the film surface and a shear horizontal resonance (SHR) polarized in the plane of the surface. The observation in light scattering of guided excitations arise from the strong elasto-optic properties of the GaN thin films as well as the presence of AlN that acts as a barrier by reducing energy leakage to the substrate. Calculations of the mode density and displacements disclose characteristics of the LGR and SHR and account for their localization and polarization features. Several of the principal elastic constants of the GaN layer are determined from the data that also reveal the bulk acoustic phonons and the Rayleigh surface mode.

DOI: 10.1103/PhysRevB.63.205302 PACS number(s): 68.35.Gy, 78.35.+c, 62.30.+d

INTRODUCTION

Recent improvements in material processing techniques and contact technology for GaN-based material systems have led to rapid progress in the fabrication of GaN optoelectronic and electronic devices.[1–3] The growth of GaN in specific polar directions is also conducive to exploiting their lattice polarization effects that are uniquely suited for applications in high-temperature piezoelectronics and as pyroelectric sensors. In fact the piezoelectric constants of GaN, while being 4–5 times larger than those of GaAs, are comparable to those of more traditional piezoelectric materials such as AlN and ZnO.[4] These characteristics have led to the growth and applications of $GaN/Al_xGa_{1-x}N$ heterolayer structures.[5–8] The growth of GaN on AlN also provides an avenue for the epitaxial growth of the dominant hexagonal GaN polytype onto Si substrates—a highly desirable feature for merging the advantages of the nitride material to the Si-based electronic industry.[9] This important step was recently realized through deposition of either a single AlN layer or AlN/3C-SiC bilayers to grow thick GaN films on Si.[10] In this paper we report on the acoustic properties of GaN/AlN heterostructures and show that, for a given GaN film thickness, the AlN layer also provides an active, high-frequency, acoustic barrier that leads to enhanced localization of specific guided acoustic excitations to the GaN layer. Observation of such surface and near-surface guided excitations by Brillouin light scattering enables several of the principal elastic constants of the supported GaN layer to be determined nondestructively in a straightforward backscattering geometry.

EXPERIMENTAL DETAILS

The single-crystal GaN layers were grown *in situ* in a chemical vapor deposition (CVD) reactor described elsewhere[10] on a sequence of designed buffer layers of 3C-SiC(200 nm) and 2H-AlN(200 nm) on Si(111) substrate. In some instances the SiC seed layer was eliminated with the AlN grown directly on silicon. The GaN film was grown on top of AlN at 1050 °C using trimethylgallium and ammonia. The thicknesses of the two GaN layers described in this work were 1300 and 500 nm and were, respectively, grown with and without the SiC buffer layer. The hcp structure of the GaN film and the (0001) film orientation were confirmed by x-ray diffraction scans as shown in Fig. 1 for one GaN/AlN/SiC/Si stack. The figure shows that only (0002) and (0004) planes of GaN and AlN are present without direct evidence of any other plane in the diffraction pattern. The ⟨0001⟩ axis of the GaN and AlN films is parallel to the [111] axis of the Si. The crystal perfection of the GaN films was analyzed by x-ray double diffraction and was slightly better than that obtained from a 2.1-μm-thick GaN film grown on sapphire with the same reactor. The in-plane

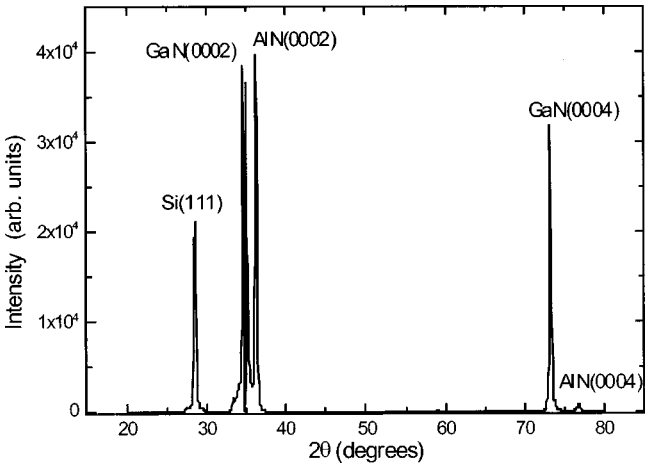

FIG. 1. X-ray diffraction scans for a GaN/AlN/SiC Si(111) structure. The peaks associated with GaN, AlN, and Si are indicated. The apparent splitting of the (0002) GaN peak is a scaling effect due to detector saturation.

(*a* and *b* axes) crystallographic relationships between the epilayers and the Si substrate was analyzed using selected-area electron diffraction and revealed the following: GaN$[1\bar{1}00]\|$AlN$[1\bar{1}00]\|3C$-SiC$[211]\|$Si$[211]$.[10] The Brillouin light scattering (BLS) measurements were performed in a backscattering geometry at room temperature with a tandem Fabry-Perot interferometer operated in a sequential six-pass configuration.[11] Approximately 100 mW of *p*-polarized $\lambda = 514.5$ nm laser radiation was used to record the polarized (*p*) and depolarized (*s*) scattered radiation; a typical measuring time for each spectrum was 15 min. The dispersion of the phonon velocities was measured by varying the magnitude of $\mathbf{q}h$, the product between the in-plane wave vector $\mathbf{q}$ and film thickness *h*, through tuning the angles of incidence θ between 40° and 80°. In order to reduce broadening of the BLS peaks arising from collecting radiation within a finite solid angle, an aperture was used to restrict the range of phonon wave vectors detected.[12] The effects of structural anisotropy on the acoustic waves were investigated by also recording the BLS spectra when the wave vector $\mathbf{q}$ was tuned from the $[1\bar{1}00]$ direction in steps of 10° through a total in-plane angle of 180°. As discussed below the observed isotropy of the in-plane wave velocity is consistent with the sixfold symmetry of the GaN lattice.

RESULTS

Figure 2 shows typical polarized $(p\text{-}p)$, depolarized $(p\text{-}s)$, and unpolarized $(p\text{-}p+s)$ Brillouin spectra below 30 GHz from the GaN(1300 nm)/AlN(200 nm)/SiC(200 nm)/Si(111) stack for angle of incidences $\theta = 60°$ and 70°. In addition to the principal Rayleigh mode (*R*) another mode, identified as the longitudinal guided resonance[13–15] (LGR) of GaN, is present in the polarized $(p\text{-}p)$ spectrum. The frequency ν of both *R* and LGR modes increases with θ and hence with wave vector $q[=(4\pi/\lambda)\sin\theta]$. Note that the intensity of the surface *R* mode is weaker than the LGR, which is a manifestation of the strong elasto-optic properties of GaN. The low-frequency $p\text{-}s$ spectra reveal the presence of the mode labeled SH that corresponds, as discussed below, to the in-plane polarized acoustic wave.[16] The frequency of this mode is also dispersive and occurs at a frequency slightly above the Rayleigh excitation. The unpolarized $(p\text{-}p+s)$ spectrum reflects a superposition of the three excitations (*R*,SHR,LGR). Figure 3 illustrates typical spectra in the high-frequency range up to 80 GHz, recorded in the same backscattering geometry as the low-frequency modes shown in Fig. 2. Two additional modes—a strong peak at 71 GHz identified with the bulk longitudinal acoustic (LA) phonon and a very weak excitation at 39 GHz associated with the bulk transverse (TA) phonon—are now evident. The lower frequency peak (23 GHz) in Fig. 3 corresponds to the LGR in Fig. 2. In contrast to the low-lying excitations, the frequency of the bulk modes is essentially insensitive to the angle of incidence. Similar spectra were observed from the other GaN/AlN/Si sample.

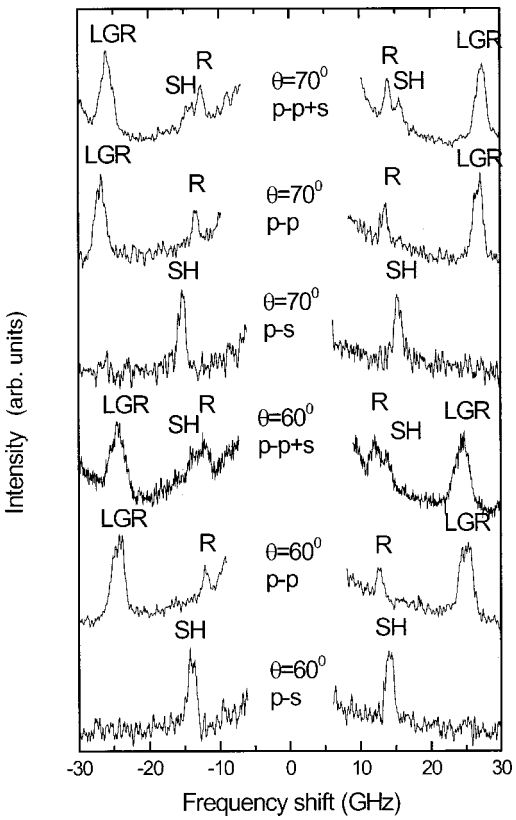

FIG. 2. Low-frequency Brillouin light scattering spectra recorded in backscattering from GaN/AlN/SiC Si(111) film for $p\text{-}p$, $p\text{-}s$, and $p\text{-}p+s$ polarizations. LGR labels the longitudinal guided resonance, SH the shear horizontal mode, and *R* the Rayleigh mode. The angle of incidence θ is as indicated and the thickness of the GaN layer is 1.3 μm.

ANALYSIS AND DISCUSSION

In order to gain insight into the character of the LGR and SH modes, the local density of phonon modes $n_i(\omega^2,q,z)$ was evaluated within a Green's-function formalism.[17] Here $i(=1-3)$ identifies the mode polarizations, where $i=3,2$ are, respectively, the sagitally polarized transverse and shear horizontal modes and $i=1$ is the longitudinally polarized mode, $\omega(=2\pi\nu)$ the angular mode frequency, and *z* the distance from the film-substrate interface where the mode density is calculated. In analyzing the response function of the sample consisting of the stack of GaN/AlN/Si layers we evaluate the response (i.e., elastodynamic Green's function) of the medium to the presence of a fictitious driving δ force *F* acting at the sample surface $z=-h$. The mode density is given by the imaginary part of the corresponding Green's tensor $G_{ii}(\omega^2,q)$. In evaluating $G_{ii}(\omega^2,q)$ we follow our previous work[15] that was based on a method proposed by Every and co-workers.[17] The elastic constants and density utilized for the AlN layer were taken from Ref. 18.

The local longitudinal, shear horizontal, and transverse density of states (DOS) were determined by, respectively, evaluating $G_{11}(\omega^2,q)$, $G_{22}(\omega^2,q)$, and $G_{33}(\omega^2,q)$ as a function of frequency for the sample stack GaN(1300 nm)/AlN(200 nm)/Si(111). The angle of incidence utilized in this calculation was 60°. In order to account for instrumental

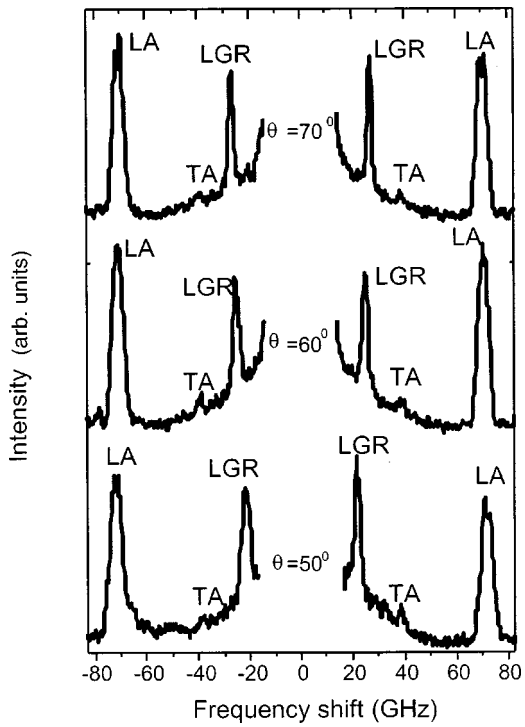

FIG. 3. High-frequency Brillouin spectra recorded in backscattering geometry from GaN/AlN/SiC/Si(111) ($h=1.3\,\mu$m). LA and TA label the bulk longitudinal and bulk transverse modes respectively. LGR is the longitudinal guided resonance.

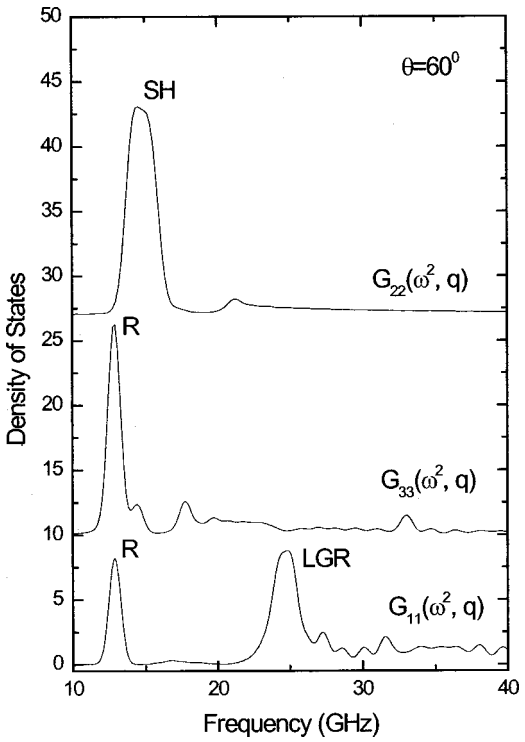

FIG. 4. Calculated local density of states as a function of frequency for GaN/AlN/Si(111) after convoluting with a Gaussian with a full width at half maximum of 0.3 GHz. The G_{33} and G_{22} are the sagittal and transverse horizontal components, respectively, and G_{11} is the longitudinal component.

broadening, each peak in the DOS was convoluted with a Gaussian with a full width at half maximum of 0.3 GHz. The results for the convoluted DOS are shown in Fig. 4. Note that the presence of a resonance in the longitudinal DOS$[G_{11}(\omega^2,q)]$ at approximately 25 GHz is in excellent agreement with the frequency shift of LGR observed in the experimental spectra (Figs. 2 and 3). The mode velocity $V_L^{\mathrm{LGR}}[=\lambda\nu/(2\sin\theta)]$ deduced for the LGR from these data corresponds to the in-plane longitudinal sound velocity and allows for a direct determination of C_{11} as we will discuss later. Furthermore, consistent with measurements, the calculated velocity V_L^{LGR} shows little dispersion with the angle of incidence in these relatively thick films.

Figure 5 shows the calculated spatial displacement field (squared) at 25.2 GHz, the frequency of the LGR in the 1300-nm GaN film at $\theta=60°$. Confirming our assignment of this mode to a guided resonance, the displacements are dominantly longitudinal in character and localized in the GaN film. Being principally longitudinally polarized, the light scattering associated with LGR is mediated primarily by the elasto-optic properties of GaN. The longitudinal displacement amplitude U_1 is found to attenuate sharply in the AlN layer prior to emerging as a very weak component in the Si substrate. The shear horizontal and sagittal transverse displacements U_2 and U_3 associated with LGR in the GaN layer are significantly weaker than U_1. The feeble displacement components within the substrate indicate that they carry little mode energy away from the film, causing negligible decay of the mode with distance. This localization of the LGR to the GaN layer accounts for its observation as a relatively sharp peak in the Brillouin spectra. In order to illustrate the effect of the AlN layer on the localization of LGR, the inset to Fig. 4 shows the calculated displacement field in the absence of the AlN layer. It is clear that, in this case, the larger relative displacement fields inside the sub-

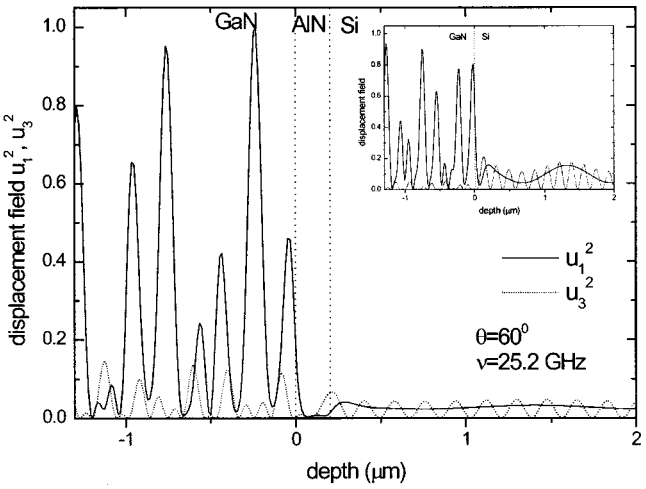

FIG. 5. Calculated spatial distributions of the square displacement field at 25.2 GHz for the LGR in 1.3-μm GaN film. The solid line represents the longitudinal component (U_1^2) while the dotted line is the transverse component (U_3^2). Note the localization and polarization of the displacement fields inside the film. The inset shows the same calculation when the AlN layer is removed.

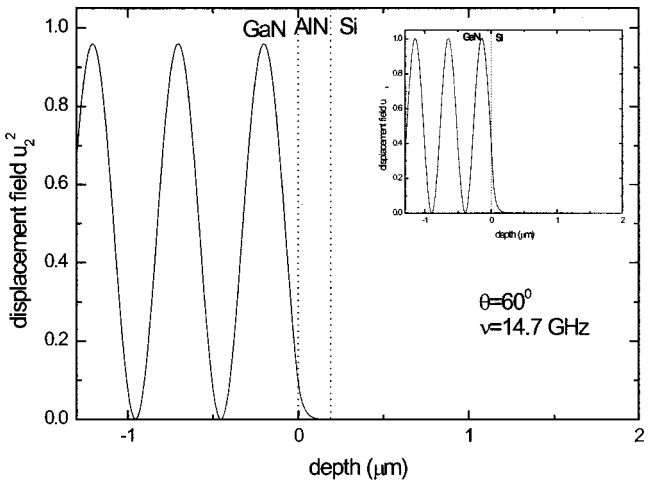

FIG. 6. Calculated spatial distributions of the square displacement field (U_2^2) at 14.7 GHz for the SH mode in the 1.3-μm GaN film. The longitudinal and sagittal transverse components (U_3^2, U_1^2) are several orders of magnitude weaker at this frequency. The inset shows the same calculation when the AlN layer is removed. Note the rapid decrease of the displacement field at the GaN/AlN or GaN/Si interface. This suggests that either AlN or Si could play the role of an acoustic barrier for the SH mode.

strate associated with both transverse and longitudinal components would lead to greater energy transmission into the substrate. In particular, since the phase velocity of the longitudinal resonance ($V_L^{\mathrm{LGR}}=7264$ m/s) satisfies the condition $V_T^{\mathrm{Si}}<V_L^{\mathrm{LGR}}<V_L^{\mathrm{Si}}$ viable decay channels exist in the Si substrate, leading to the finite partial components evident in the inset to Fig. 5. Here V_T^{Si} and V_L^{Si} are the transverse and longitudinal acoustic phonon velocities of Si. On the other hand, the AlN layer has a significant effect on the localization of the LGR to the GaN layer since it minimizes the coupling of partial wave components within the nitride layer with those that radiate energy into the substrate. We note that the extent of the leakage of the LGR into the Si substrate will, for a given AlN thickness, also depend on the thickness of the GaN layer. Such behavior is due to the oscillatory dependence of the LGR localization on the GaN thickness.[13]

The sharp resonance at 12 GHz in the calculated G_{11} and G_{33} components of the DOS (Fig. 4) corresponds to the Rayleigh excitation *R* observed in *p-p* scattering. In transparent materials such as GaN, the effective mechanism mediating the light scattering from the Rayleigh mode is elasto-optic coupling, while the ripple mechanism, which provides the primary coupling in opaque systems, contributes weakly. In contrast to the Rayleigh mode there have been only few reports[16] on the observation of the guided shear horizontal excitation that is polarized parallel to the surface, as evident in the DOS $[G_{22}(\omega^2,q)]$ in Fig. 4. In this work we assign the mode labeled SH (Fig. 2) in the *p-s* scattering spectra to this excitation. The calculated DOS $[G_{22}(\omega^2,q)]$ correctly reproduces this feature (Fig. 4). The displacement fields associated with the shear horizontal mode are illustrated in Fig. 6. The results confirm that at the frequency of the SH mode (14.7 GHz at $\theta=60°$) there is a strong shear (in-plane) displacement field U_2 associated with the wave. The longitudinal displacement component is, by contrast, smaller by several orders of magnitude. Again, it is evident from the variation of the displacement fields with depth (Fig. 6) that the AlN layer provides an effective means to localize the SH mode to the GaN layer. We also studied the effect of removing the AlN layer, and the results are shown in the inset to Fig. 6. A dramatic decrease in the shear displacement field is evident near the GaN/Si interface with the profile of the shear displacement field being similar to that when the AlN layer is present. This suggests that either the Si substrate or the AlN intermediate layer can act as an effective acoustic barrier to the SH resonance. For the SH mode all partial components of the displacement field decay inside the substrate since the SH mode phase velocity, $V_{\mathrm{SH}}=4160$ m/s, is smaller than the transverse and longitudinal velocity, $V_T^{\mathrm{Si}}=5844$ m/s and $V_L^{\mathrm{Si}}=8433$ m/s of Si.

The spectra recorded in backscattering at a larger free spectral range shows peaks associated with the bulk acoustic excitations. In particular, in Fig. 3, the bulk LA mode and the very much weaker TA peak occurs, respectively, at 71 and 39 GHz. Thus five distinct excitations (the LGR, SHR, Rayleigh mode, bulk LA, and bulk TA) are observed in the backscattering geometry in these BLS experiments. The first three excitations propagate parallel to the surface, while the latter two are phonons whose propagation direction is, due to the relatively large refractive index of GaN, essentially normal to the film surface. Given the distinctive polarization features of the two guided modes they directly allow for the elastic constants C_{11} ($=321\pm3$ GPa) and C_{66} ($=105\pm2$ GPa) to be determined from the mode velocity $[(C_{jj}/\rho)^{1/2}]$ for a given *q*. The values of $n=2.44$ and $\rho=6.09$ g/cm^3 were utilized for the refractive index and density respectively.[1,19] The peak position of the bulk TA and LA modes allow for a direct determination of $C_{44}=103\pm2$ GPa and $C_{33}=342\pm2$ GPa via the relations $C_{ii}=[\lambda\nu/(2n)]^2\rho$. The lack of anisotropy in the mode frequencies as the direction of **q** was varied in the film plane is consistent with the hexagonal symmetry of the GaN surface; the isotropy condition $C_{66}=[C_{11}-C_{12}]/2$ leads to $C_{12}=111\pm2$ GPa.

Previous BLS experiments on GaN have mainly focused on the bulk material[20,21] with one report on measurements from an epitaxial film.[22] These experiments on bulk samples utilized several scattering geometries that included transmission through the sample, 90° scattering, and, as in the present study, in backscattering. These configurations of the bulk samples enabled coupling to excitations propagating parallel to the surface with sagittal and shear horizontal polarizations. We note that while the value of C_{44} agrees with that of the bulk, the C_{11}, C_{66}, and C_{33} values deduced in this study for the GaN films are about 20% smaller than those of the bulk crystals. Reasons for this discrepancy between the elastic constants bulk and thin films are unclear at present and may be related to differences in density and the presence of stresses in the thin films. Such differences between elastic constants of bulk and thin films have been reported in other systems.[23]

Information on the elastic constants of thin GaN films is valuable where a major problem in their growth is the large misfit stress that appears at the GaN substrate interface.

Knowledge of the elastic constants is crucial in determining interface stresses and stress distributions that develop in GaN. Correctly evaluating these stresses is important both for assessing GaN film quality and for estimating strain-induced energy-band shifts at the film/substrate interface and $Al_xGa_{1-x}N$/GaN heterointerface that influence the electric properties of GaN-based devices. For instance, due to the large GaN piezoelectric constants, strain-induced electric fields would lead to spatial separation of electrons and holes in $Al_xGa_{1-x}N$/GaN quantum wells.[4,7,8] This in turn can strongly affect the performance of light-emitting devices based on III-N quantum-well structures.

CONCLUSIONS

In summary, we have reported on the observation in Brillouin light scattering of a longitudinal guided resonance and of a shear horizontal resonance in $2H$-GaN films grown on AlN films deposited on Si. Theoretical simulations based on evaluating the elastodynamic Green's tensor reveal the properties of these resonances and emphasize the role of the AlN layer that acts as an acoustic barrier to these high-frequency modes and that augments their localization inside the GaN layer. In addition, bulk LA and TA phonons as well as the surface Rayleigh excitation is observed. Observation of several distinct excitations in a single backscattering experiment has also allowed for four of the five independent elastic stiffness constants (C_{11}, C_{44}, C_{66}, and C_{33}) of the GaN layer to be determind.

The work at the Ohio State University was supported by the Army Research Office under Grants No. DAAD 19-00-1-0396 and No. DAAG 55-97-1-0260.

[1] *Wide Band Gap Semiconductors*, edited by T. D. Moustakas, J. H. Pankove, and Y. Hamakawa, Mater. Res. Soc. Symp. Proc. No. 242 (Materials Research Society, Pittsburgh, 1992).
[2] S. Strite and M. Morkoc, J. Vac. Sci. Technol. B **10**, 1237 (1994).
[3] J. T. Glass, B. A. Fox, D. L. Dreifus, and B. R. Stoner, MRS Bull. **23**, 49 (1998).
[4] A. D. Bykhovski, B. L. Gelmont, and M. S. Shur, J. Appl. Phys. **81**, 6332 (1997).
[5] A. Bykhovski, B. Gelmont, and M. S. Shur, J. Appl. Phys. **74**, 6734 (1993).
[6] R. Gaska, J. Yang, A. D. Bykhovski, M. S. Shur, V. V. Kaminski, and S. M. Soloviev, Appl. Phys. Lett. **72**, 64 (1998).
[7] P. M. Asbeck, E. T. Yu, S. S. Lau, G. J. Sullivan, J. Van Hove, and J. M. Redwing, Electron. Lett. **33**, 1230 (1997).
[8] E. T. Yu, G. J. Sullivan, P. M. Asbeck, C. D. Wang, D. Qiao, and S. S. Lau, Appl. Phys. Lett. **71**, 2794 (1997).
[9] H. M. Liaw, R. Venugopal, J. Wan, R. Doyle, P. Fejes, M. J. Loboda, and M. R. Melloch, in *Proceedings of the International Conference On Silicon Carbide and Related Materials*, North Carolina, 1999, edited by Calvin H. Carter, Jr., Robert P. Devaty, and Gregory S. Rohrer (Trans Tech Publications, Switzerland, 2000), pp. 1463–1466.
[10] H. M. Liaw, R. Venugopal, J. Wan, R. Doyle, P. L. Fejes, and M. R. Melloch, Solid-State Electron. **44**, 685 (2000).
[11] J. R. Sandercock, in *Light Scattering in Solids III*, edited by M. Cardona and Guntherodt (Springer, Berlin 1982), p. 173.
[12] P. R. Stoddart, J. C. Crowhurst, A. G. Every, and J. D. Comins, J. Opt. Soc. Am. B **15**, 2481 (1998).
[13] B. Hillebrands, S. Lee, G. I. Stegeman, H. Cheng, and J. E. Potts, Phys. Rev. Lett. **60**, 832 (1988).
[14] F. Nizzoli, C. Byloos, L. Giovannini, C. E. Bottani, G. Ghislotti, and P. Mutti, Phys. Rev. B **50**, 2027 (1994).
[15] M. Chirita, R. Sooryakumar, H. Xia, O. R. Monteiro, and I. G. Brown, Phys. Rev. B **60**, R5153 (1999).
[16] J. A. Bell, R. J. Zanoni, C. T. Seaton, G. I. Stegeman, W. R. Bennett, and C. M. Falco, Appl. Phys. Lett. **51**, 652 (1987); C. E. Bottani, G. Ghislotti, and P. Mutti, J. Phys.: Condens. Matter **6**, L85 (1994).
[17] A. G. Every, K. Y. Kim, and A. A. Maznev, J. Acoust. Soc. Am. **102**, 1346 (1997); X. Zhang, J. D. Comins, A. G. Every, P. R. Stoddart, W. Pang, and T. E. Derry, Phys. Rev. B **58**, 13677 (1988).
[18] C. Deger, E. Born, H. Angerer, O. Ambacher, M. Stutzmann, J. Hornsteiner, E. Riha, and G. Fischerauer, Appl. Phys. Lett. **72**, 2400 (1998).
[19] E. Ejder, Phys. Status Solidi A **6**, 445 (1971).
[20] A. Polian, M. Grimsditch, and I. Grzegory, J. Appl. Phys. **79**, 3343 (1996).
[21] M. Yamaguchi, T. Yagi, T. Azuhata, T. Sota, K. Suzuki, S. Chichibu, and S. Nakamura, J. Phys.: Condens. Matter **9**, 2412 (1998).
[22] Y. Takagi, M. Ahart, T. Azuhata, T. Sota, K. Suzuki, and S. Nakamura, Physica B **219&220**, 547 (1996).
[23] W. Pang, A. G. Every, J. D. Comins, P. R. Stoddart, and X. Zhang, J. Appl. Phys. **86**, 311 (1999).